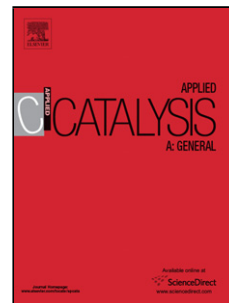


Accepted Manuscript

Title: Effect of the support on the catalytic stability of Rh formulations for the water-gas shift reaction

Authors: Carolina A. Cornaglia, John F. Múnera, Laura M. Cornaglia, Eduardo A. Lombardo, Patricio Ruiz, Alejandro Karelavic



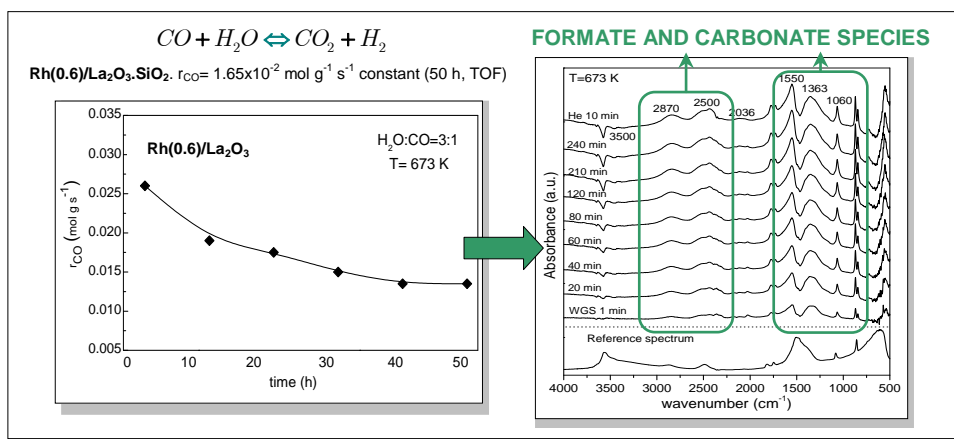
PII: S0926-860X(12)00323-7
DOI: doi:10.1016/j.apcata.2012.05.042
Reference: APCATA 13705

To appear in: *Applied Catalysis A: General*

Received date: 1-2-2012
Revised date: 10-5-2012
Accepted date: 26-5-2012

Please cite this article as: C.A. Cornaglia, J.F. Múnera, L.M. Cornaglia, E.A. Lombardo, P. Ruiz, A. Karelavic, Effect of the support on the catalytic stability of Rh formulations for the water-gas shift reaction, *Applied Catalysis A, General* (2010), doi:10.1016/j.apcata.2012.05.042

This is a PDF file of an unedited manuscript that has been accepted for publication. As a service to our customers we are providing this early version of the manuscript. The manuscript will undergo copyediting, typesetting, and review of the resulting proof before it is published in its final form. Please note that during the production process errors may be discovered which could affect the content, and all legal disclaimers that apply to the journal pertain.



Highlights

- Catalysts for high temperature water gas shift reaction in membrane reactors.
- Rhodium over La_2O_3 and $\text{La}_2\text{O}_3/\text{SiO}_2$ oxides as catalysts.
- Deactivation of the Rh/ La_2O_3 solid due to the formation of carbonate/formate species.
- The initial activity is restored after being burnt in air at 673 K.

Accepted Manuscript

Effect of the support on the catalytic stability of Rh formulations for the water-gas shift reaction

Carolina A. Cornaglia⁽¹⁾, John F. Múnera⁽¹⁾, Laura M. Cornaglia⁽¹⁾, Eduardo A. Lombardo^{(1)}, Patricio Ruiz⁽²⁾, Alejandro Karelovic⁽²⁾*

⁽¹⁾Instituto de Investigaciones en Catálisis y Petroquímica (FIQ, UNL-CONICET) –INCAPE-
Santiago del Estero 2829-3000 Santa Fe, Argentina.

⁽²⁾Institute of Condensed Matter and Nanoscience - IMCN, Division Molecules Solids and Reactivity –
MOST. Université Catholique de Louvain,
Place Croix du Sud 2/1, 1348, Louvain-la-Neuve, Belgium

*E-mail: nfisico@fiq.unl.edu.ar

Tel/ fax: 54-342-4536861

Abstract

The stability of Rh(0.6)/La₂O₃ and Rh(0.6)/La₂O₃(27).SiO₂ catalysts used in the water-gas shift reaction (WGS) was studied. In order to understand the different behavior of the two formulations, XRD, Raman spectroscopy and operando-DRIFTS were employed. It was demonstrated that Rh/La₂O₃.SiO₂ showed a constant activity after 50 h on stream and that it was made up of La₂Si₂O₇ with very low crystallinity and SiO₂. On the other hand, Rh/La₂O₃ after use evolved to a mixture of oxycarbonates and lanthanum hydroxide evidenced by XRD and confirmed by Raman spectroscopy. This solid suffered a significant deactivation which was assigned to the formation of very small amounts of formate and carbonate residues. These residues disappeared after being burnt in air at 673 K and the initial catalytic activity was restored. The results obtained were useful to explain the reasons for the different stability of the two formulations and could have implications for the design of active catalysts used in the WGS and in the processes in which it is involved.

Keywords: hydrogen purification, formate species, binary support, deactivation

1. Introduction

The water–gas shift (WGS) reaction, $\text{CO} + \text{H}_2\text{O} \leftrightarrow \text{CO}_2 + \text{H}_2$, is an important step in several industrial processes [1,2]. It is used to increase hydrogen production and remove CO before ammonia synthesis in refinery hydroprocesses, or to adjust the H_2/CO molar ratio in methanol production and Fischer–Tropsch synthesis.

The WGS reaction is one of the key steps in a typical fuel processor (FP) used in CO-free hydrogen production. The WGS reaction unit in a FP follows the reformer and reduces the CO concentration while increasing the hydrogen yield. Since the reversible WGS reaction is moderately exothermic and equilibrium-limited, lower CO levels can be achieved at low temperatures. Nevertheless, high temperatures are required to increase the reaction rate. In a FP, the WGS reaction is normally performed in two serial reactors, namely the high-temperature shift reactor operating at 623–773 K, and the low-temperature shift reactor operating at 453–513 K for obtaining high activity and conversion simultaneously [3]. In order to obtain H_2 containing < 10 ppm CO for use in PEM fuel cells, a second purification step is needed (COPrOx or PSA).

An attractive alternative is to conduct the WGS reaction in a membrane reactor. In this way, only one vessel is needed and the CO conversion increases above equilibrium value leaving behind a stream rich in CO_2 ready for sequestration. The catalyst needed to achieve this goal should operate at ca. 670 K to strike a balance between the negative effect of CO upon H_2 permeability [4] and the palladium membrane durability. Both factors decrease with temperature.

To optimize the reactor operation, a high-temperature, active, stable catalyst is required. The new formulation should not form carbonaceous residues because carbon has a great Pd affinity which rapidly destroys the membrane.

Several commercial formulations are available to conduct the reaction at low or high temperature [5]. There has been great interest in the development of active, selective, thermally stable, poison-resistant, non-pyrophoric noble-metal based WGS reaction catalyst formulations supported on metal oxide carriers. They exhibit much faster high-temperature kinetics compared to conventional ones and offer

other significant advantages such as no need of activation prior to use, no degradation on exposure to air or temperature cycles, which could result in the reduction of reactor size and other costs. Note that in FP, the WGS reactors using commercial HT catalysts are the largest ones [6]. This is another factor that stimulates the search for more active catalysts. Among the noble metals, Pt and Rh are the best candidates. Rh has been selected for the present study due to its excellent performance in the dry reforming of methane [7] where the WGS reaction is also present. In addition, it is well known that supported Rh catalysts are very active in the partial oxidation of methane; they also play an important role in modulating the H₂/CO molar ratio in the WGS reaction. Moreover, today the price of Rh is very similar to that of Pt.

A previous study of the WGS reaction over Rh supported on La₂O₃-containing formulations [8] showed that at 673 K, the CO rate was constant for at least 50 h for the Rh(0.6)/La₂O₃(27).SiO₂ catalyst while Rh(0.6)/La₂O₃ suffered a progressive deactivation. For the stable Rh/La₂O₃.SiO₂ solid, a kinetic study demonstrated that the data recorded at temperatures between 598 and 723 K were well-fitted by a physically meaningful L-H kinetics. However, since the initial reaction rate for the La₂O₃ supported catalyst was ca. 60% higher than the La₂O₃.SiO₂ based catalyst, there is a driving force to understand the nature of the deactivation process of the Rh(0.6)/La₂O₃ catalyst that could lead to the design of better catalysts for the WGS reaction.

Through qualitative or semi quantitative methods, several authors have reported that the deactivation causes of WGS formulations may be broadly due to: i) loss of metal surface area (sintering) [9], ii) chemical transformation of support materials and/or catalysts [10], iii) carbon deposition (reactant species decomposition) [11], iv) formation of carbonate/formate species [12, 13].

In the present study, we investigated the role of these deactivation agents in the slow performance decay of the Rh(0.6)/La₂O₃ catalyst and why they did not develop when Rh(0.6)/La₂O₃(27).SiO₂ was used. With this goal in mind both fixed-bed reactor measurements and “operando” DRIFT experiments were performed. The use of the latter technique is particularly important because the formation of the different species adsorbed on the surface of the catalysts can be studied in real time, thus making it

possible to investigate the influence of these adsorbed species on the deactivation process. In this work, the influence of water, CO and O₂ in the gas atmosphere was studied using these two techniques. In addition XRD, FTIR and Laser Raman spectroscopies were used to characterize the fresh and used (in WGS reaction) solids.

2. Experimental

2.1. Catalyst preparation

The Rh(0.6)/La₂O₃ catalyst (containing 0.6 wt% Rh) was prepared by the conventional wet impregnation of La₂O₃ (Alfa Aesar, 99.99%) using RhCl₃·3H₂O (Alfa Aesar, 99.99 %). Initially, the salt of RhCl₃·3H₂O (30.8 mg) was dissolved in 10 ml of deionized water and then La₂O₃ was added. The resulting mixture was stirred during 5 h and heated at 353 K to evaporate the water. The solid material was dried in an oven at 383 K overnight.

The La₂O₃.SiO₂ support was prepared by the incipient wetness impregnation of SiO₂ (Aerosil 200) with lanthanum nitrate (Sigma Aldrich, 99.9%). SiO₂ was previously calcined at 1173 K. The loading was 27.0 wt% of La₂O₃. Initially, La(NO₃)₃ was dissolved in deionized water (calculated to obtain an incipient wetness impregnation) and then SiO₂ was added. The mixture obtained was homogenized for about 45 min. The sample was kept at room temperature for 2 hours and then dried at 383 K overnight. The resulting solid was calcined at 823 K.

The Rh(0.6)/La₂O₃(27).SiO₂ catalyst was prepared by incipient wetness impregnation. The salt of RhCl₃·3H₂O was dissolved in deionized water (calculated to obtain an incipient wetness impregnation). The La₂O₃.SiO₂ support was added and the mixture was homogenized during 45 min. The sample was kept at room temperature for 2 hours and then dried at 383 K overnight. Both catalysts, independently of the preparation method or the support employed, were calcined for 6 h at 823 K in flowing air.

2.2. Catalyst characterization

2.2.1. Metal dispersion

The Rh dispersion of the fresh catalysts, following the H₂ reduction at 773 K for 2 h, was determined by static equilibrium adsorption of H₂ at 298 K in a conventional vacuum system.

2.2.2. X-ray diffraction (XRD)

The XRD patterns of the calcined and used solids were obtained with an XD-D1 Shimadzu instrument, using Cu K α radiation at 30 kV and 40 mA. The scanning rate was 1.0°/min for values between $2\theta = 10^\circ$ and 60° .

2.2.3. FTIR and Laser Raman (LRS) spectroscopies

The IR spectra were obtained using a Smiths Illuminativ II JY spectrometer with a spectral resolution of 8 cm⁻¹, and employing pressed disks of pure sample powders (15 mg). The Raman spectra were recorded using a LabRam spectrometer (Horiba-Jobin-Yvon) coupled to an Olympus confocal microscope (a 100X objective lens was used for simultaneous illumination and collection), equipped with a CCD detector cooled to about 200 K using the Peltier effect. The excitation wavelength was in all cases 532 nm (diode-pumped solid-state laser). The laser power was set at 30 mW.

2.2.4. Operando DRIFTS

Diffuse Reflectance Infrared Fourier-Transform Spectroscopy was performed with a Bruker Equinox 55 infrared spectrometer equipped with an air cooled MIR source with KBr optics and a MCT detector. Spectra were obtained by collecting 200 scans with a resolution of 4 cm⁻¹. The catalysts were placed without packing or dilution inside a cell with controlled temperature and environment (Spectra-Tech 0030-102) equipped with ZnSe windows. The reference spectrum for each experiment was taken when the catalysts was under He right before the introduction of reactive gases. The gases at the outlet of the cell were analyzed by a quadrupole mass spectrometer (Balzers QMS 200) following the evolution of $m/z = 2$ (H₂), 18 (H₂O), 28 (CO) and 44 (CO₂).

The catalysts used in these experiments were previously reduced under hydrogen flow (30 ml min^{-1}) in a fixed-bed reactor at 673 K for 1h and then grounded finely, before the infrared experiments. Then the catalyst was placed in the DRIFTS cell. Before analysis, the cell was flushed with He (20 ml min^{-1}) for 10 min and then reduced again in a stream of H_2 (10 vol. %) in He (20 ml min^{-1}), during 1h at 1 atm and 673 K. The flow was switched to He, the temperature adjusted to the desired value and then the reactive mixture was fed to the sample. (1.1% H_2O + 1.1% CO + balance He).

2.3. Catalytic tests

The WGS reaction was studied using a conventional catalytic fixed-bed tubular reactor (5 mm i.d.) isothermally operated at atmospheric pressure. The feed stream gas mixture was controlled using MKS mass flow controllers; steam was generated in a preheater (623 K) fed with deionized water from a syringe pump (Apema S.R.L.) at the desired flow rate. The reaction temperature was measured through a sliding thermocouple placed inside the catalyst bed. The catalysts (8 mg) were diluted with inert powder quartz (1:4) to avoid channeling effects. The solids were ground and sieved down to $150 \mu\text{m}$ (100 mesh) and the total gas flow rate was 600 ml min^{-1} to ensure conditions of chemical control. Before use the catalysts were heated in Ar (Linde, 5.0) at 673 K and then reduced in situ in flowing H_2 (50 ml min^{-1}) (Indura S.A., 5.0) at the same temperature for 2 h. CO (Indura S. A., 2.3) was used.

The gases leaving the reactor flowed through an ice-cooled trap and a tube packed with silica gel to remove water before the gas chromatographic analysis. The feed and product streams were analyzed with a Shimadzu 9A (TCD) gas chromatograph equipped with a Hayesep D column for the complete separation of the gaseous components. All the reaction rates were calculated from data obtained with the reactor being operated in differential mode and in chemical regime.

As regards the approach to equilibrium of the WGS reaction, one can define a fraction of reaction equilibration (η) using the following equation:

$$\eta = \frac{1}{K_{eq}} \frac{P_{CO_2} \cdot P_{H_2}}{P_{CO} \cdot P_{H_2O}} \quad (1)$$

where P_i is the measured partial pressure of reactants and products and K_{eq} is the equilibrium constant calculated at the corresponding reaction temperature.

The differential reaction rate $(-r_{CO})^o$ [$\text{mol g}^{-1} \text{s}^{-1}$] was calculated as

$$(-r_{CO})^o = \frac{X_{CO}}{W_C / F_{CO}^o} \quad (2)$$

where W_C is the catalyst mass and F_{CO}^o is the molar flow rate of the fed CO.

For the reaction rates measurements, CO conversions were always below 10% and $\eta < 0.001$.

3. Results and Discussion

3.1. Stability tests

The stability of both catalysts was evaluated flowing a stream of 9% CO, 27% H₂O, 64% Ar (H₂O:CO=3:1) at 673 K over the reduced solid. The Rh(0.6)/La₂O₃(27).SiO₂ formulation showed a constant reaction rate of $1.65 \times 10^{-4} \text{ mol g}^{-1} \text{ s}^{-1}$ ($\text{mol CO}_{\text{converted}} \text{ g}_{\text{catalyst}}^{-1} \text{ s}^{-1}$) during at least 50 h. Furthermore, this catalyst was also stable for more than 50 h when the reactor was operated in integral regime (Not shown). In the same period, the Rh(0.6)/La₂O₃ catalyst lost 51 % of its initial activity (Table 1).

The initial TOFs of both catalysts were calculated by H₂ chemisorption and are shown in Table 2. Note that Rh/La₂O₃ has a lower Rh dispersion than Rh/La₂O₃.SiO₂. This low dispersion indicates a different Rh particle size that could affect the metal reduction. However, Duprez et al [14] found that the rhodium reduction is not very dependent on particle size. Furthermore, for the Rh/La₂O₃ catalyst, Irusta et al [15] reported that the rhodium is completely reduced at temperatures below 523 K.

Vidal et al [16] and later Irusta et al [15] have already shown that Rh/La₂O₃.SiO₂ solids show high metal dispersion. There have been speculations about the reasons behind this observation but no definite proofs have been provided. The lower Rh dispersion on La₂O₃ might be related to the strong metal

support interaction [15] that might be symptomatic of a certain extent of surface coverage of the metal clusters by La_2O_3 .

The TOF values of several other catalysts are reported in Table 2. These catalysts have been tested by Panagiotopoulou and Kondarides [17] under operating conditions similar to ours, feeding only CO and water as reactants, 3% CO, 10% H_2O (balance He). Note that the TOFs of our catalysts are 1-2 orders of magnitude higher than the others included in Table 2. We were not able to find comparable TOF data from other sources because most of the data reported with noble metals, generally supported on reducible oxides, have been obtained at lower temperatures

3.2. Characterization of fresh and used catalysts

Table 3 shows the results obtained by XRD and LRS analysis. In the fresh $\text{Rh}/\text{La}_2\text{O}_3$ solid, XRD mainly reveals the presence of $\text{La}(\text{OH})_3$ (ASTM No. 6-585), although traces of oxycarbonates are also detected. After being on reacting stream at 673 K for 24 h, the diffractogram showed only the presence of hexagonal $\text{La}_2\text{O}_2\text{CO}_3$ (type II, ASTM No. 37-804).

The XRD patterns of fresh and used $\text{Rh}(0.6)/\text{La}_2\text{O}_3(27).\text{SiO}_2$ are identical. These diffractograms show broad peaks centered around $2\theta = 28^\circ$ and 45° which correspond to the low crystallinity lanthanum disilicate phase $\text{La}_2\text{Si}_2\text{O}_7$ (Table 3), as previously reported by Vidal et al [18] and Irusta et al. [15]. Peaks indicating the presence of lanthanum carbonates, oxycarbonates or hydroxide are not observed before and after exposure to the reacting stream. This seems to be due to the strong interaction between SiO_2 and La_2O_3 preventing the reaction of the latter with carbon oxides to form detectable amounts of carbonates.

No XRD reflections associated with metallic Rh were detected either in the fresh or in the used catalysts.

The Raman spectra of the fresh and used $\text{Rh}(0.6)/\text{La}_2\text{O}_3$ catalysts confirm the information provided by XRD. Besides, LRS is a very sensitive tool to detect the formation of graphitic carbon deposited on solid oxides. A group of broad, very-low-intensity bands centered at 1340 and 1590 cm^{-1} are observed in

the used catalysts (Table 3). Both peaks are assigned to the presence of small amounts of graphitic carbon not detectable by TGA analysis (Detection limit of our instrument: 1×10^{-4} g/g catalyst).

The Raman spectrum of the used Rh(0.6)/La₂O₃(27).SiO₂ solid shows a weaker signal of this band than the Rh(0.6)/La₂O₃ catalyst. This allows us to suggest that, since the Rh(0.6)/La₂O₃ catalyst lost 51% of its activity after 50 h (TOS) while Rh(0.6)/La₂O₃.SiO₂ remained stable for the same period, it is unlikely that the graphitic residues could be responsible for the deactivation of the former solid. This is an important information to understand the reasons for the deactivation of Rh supported catalysts.

3.3. Operando evolution of the reacting system

3.3.1. Rh(0.6)/La₂O₃(27).SiO₂ catalyst

DRIFT spectra of the Rh(0.6)/La₂O₃(27).SiO₂ catalyst obtained during exposure to a reacting mixture (1.1% H₂O, 1.1% CO, 98.8% He) at different temperatures are shown in Figure 1a. Figure 1b reports the evolution of the mass spectrometer signals during the WGS reaction. The simultaneous slope change of the H₂ and CO₂ signals indicates that the reaction begins at ca. 550K.

The absorption band at 3750 cm⁻¹ is most likely associated with the existence of isolated silanol groups [19]. The shoulder of this band at a lower wavenumber is likely due to hydrogen bonded adjacent hydroxyls. The small band at 2350 cm⁻¹ corresponds to the gas-phase CO₂ contribution. It is observed that, at higher temperature, the intensities of the small signals at 1950, 1850, and 1630 cm⁻¹ increase. These bands correspond to the vibrations of the silica skeleton.

At low temperatures, the spectra present a doublet at 2125 and 2034 cm⁻¹ pertaining to gem-dicarbonyls. Note that these bands disappear above 573 K and a new one at 2060 cm⁻¹ assigned to CO linearly adsorbed on Rh is observed. At 673 K, this band remains unchanged even after exposure to He during 15 min at the same temperature.

For the Rh(0.6)/La₂O₃(27).SiO₂ catalyst (Fig. 1) and the La-Si support (not shown), a well-defined band at 1300 cm⁻¹ is observed. This signal that evolves similarly with temperature in both solids could not be assigned to a particular feature of these solids. Clearly this band does not belong to species

formed during WGS reaction. The presence of a negative band at 1600 cm^{-1} corresponds to adsorbed water present in the reference spectrum that decreases with increasing temperature.

3.3.2. *Rh(0.6)/La₂O₃ catalyst*

The evolution of the DRIFT spectra of the Rh(0.6)/La₂O₃ catalyst with time on stream (TOS) at 673K is shown in Figure 2. Bands at 720, 842, 864, 1060, 1363 and 1550 cm^{-1} assigned to different types of oxycarbonates are now observed [15]. These bands were not seen in the Rh(0.6)/La₂O₃(27).SiO₂ catalyst (Fig. 1).

One key feature of the reference spectrum (Fig. 2) is the presence of the two bands at 2870 and 2500 cm^{-1} in the fresh catalyst. The band at 2870 cm^{-1} has been attributed to either formate or oxycarbonate overtones [15]. Similarly, the 2500 cm^{-1} signal could be attributed to a carbonate overtone [20].

The bands at 1363 cm^{-1} and 1550 cm^{-1} may be due to the presence of either monoclinic (type Ia) oxycarbonates or formate species, or both [15]. At longer time-on-stream, the intensity of these peaks slightly increases together with the signal at 2870 cm^{-1} that increases faster. It can also be observed that a band at 2500 cm^{-1} grows together with the signal at 2870 cm^{-1} with time on stream (Fig. 2). Note that when a He stream is fed at 673 K after reaction, these signals do not disappear. These bands might be related to the Rh(0.6)/La₂O₃ deactivation. The formate could be formed on the catalyst surface due to the interaction of adsorbed CO with surface OH. This reaction was proposed on Rh/CeO₂ by Shido and Iwasawa [21] following a thorough spectroscopic characterization of the surface intermediates involved in the WGS reaction. More recently, Davis and co-workers concluded that a similar mechanism of formate formation operates on Pt/CeO₂ [22] and also on Pt/ZnO and Pt/ZrO₂ [23].

The broad absorption at approximately 3550 cm^{-1} appearing in the reference spectrum has been assigned to interacting surface hydroxyl groups in lanthana [24]. This band decreases with time on stream (Fig. 2) and increasing temperature (Fig. 3a) while the 2870 cm^{-1} band increases. This also lends support to the formation of formates on Rh/La₂O₃ through the reaction of adsorbed CO with the interacting surface hydroxyls. A very-low-intensity feature is visible at 2036 cm^{-1} . This band is

assigned to linearly adsorbed CO on metallic rhodium. No bands attributed to gem-dicarbonyl (2125 - 2034 cm^{-1}) are observed. This catalyst shows a lower Rh dispersion and surface area (Table 2) than the Rh(0.6)/La₂O₃.SiO₂.

Figure 3 shows the DRIFTS spectra obtained during the WGS reaction and the mass spectrometer signals at different temperatures on Rh(0.6)/La₂O₃. Note that the characteristic bands assigned to carbonate species (860, 1060, 1363 and 1550 cm^{-1}) increase with temperature. This effect could be due to the appearance of CO₂ as product of the WGS (Fig. 3b), and its consequent reaction with the support that increases with both higher temperature and CO₂ partial pressure. In the high-frequency range, the band at 3560 cm^{-1} decrease with temperature.

Note, that the WGS reaction begins at ca. 520 K, when the hydrogen appears as reaction product (Fig. 3b). At the same time, the two bands at 2870 and 2500 cm^{-1} develop, suggesting again that strongly held oxygenates are involved in the catalyst deactivation.

If Figures 1b and 3b are compared, it can be observed that the onset of the WGS reaction occurs at lower temperature on Rh(0.6)/La₂O₃ than on Rh(0.6)/La₂O₃(27).SiO₂. This leads to the conclusion that Rh(0.6)/La₂O₃ is more active at low time-on-stream, in agreement with the reaction rate data reported in Table 1.

3.4. Effect of H₂O, CO, inert and O₂ upon the catalytic behavior of Rh(0.6)/La₂O₃

3.4.1. Effect of water

To investigate the effect of water, a reduced sample of Rh(0.6)/La₂O₃ was exposed to a flowing reacting mixture (9% CO, 27% H₂O, 64% Ar) at 673 K during 3 h. Then, the CO flow was shut off and only H₂O and Ar were fed for 24 h. After that, the feed of carbon monoxide was reestablished.

In the first 3 hours, the deactivation of the catalyst occurred (Fig. 4). During the next 24 h only steam and Ar were fed to the reactor. Note, that when the WGS reaction conditions were reestablished the catalytic activity was almost two times faster than before. To further investigate the origins of this reactivating effect of H₂O, Figure 5 shows the IR spectra obtained after different treatments: fresh

catalyst (a), after WGS reaction for 24 h (b) and after water treatment (c). The catalyst subjected to the WGS reaction during 24 h shows bands located at 2500 and 2870 cm^{-1} whereas the fresh and the water treated solids do not show them. As already said, these bands belong to either formates or overtones of carbonates, or both. The lanthanum formates and oxycarbonates are very stable compounds at $T > 673$ K [25,26]. This may indicate that the oxygenates formed during calcination could already be present in the fresh solid but in amounts not detectable through the IR instrument used for this experiment. The high amount of adsorbed water remaining after the 24 hours of treatment may favor the decomposition of the formates being formed (vide infra), thus explaining the constant activity for ca. 3 hours observed in Figure 4. In what follows we will try to test this hypothesis.

A DRIFTS experiment was performed to further study the effect of water over the catalyst (Fig. 6). A fresh sample was introduced in the system and heated in He up to 673 K. Note that the corresponding spectrum already shows the presence of the 2870 and 2500 cm^{-1} bands (see also the background spectrum in Fig. 2). The water treatment at the same temperature shows a progressive reduction in intensity of these bands. When CO was fed together with water (upper two spectra) the intensities of these bands significantly increased and also did so the 1363 cm^{-1} band. These results are very important because they confirm: i) the presence of the 2870 and 2500 cm^{-1} bands in the fresh catalyst, ii) the simultaneous growth of the oxycarbonate/formate band at 1363 cm^{-1} with those at 2870 and 2500 cm^{-1} under the WGS reaction conditions. Note that the air stream used for calcination contains CO_2 traces that may react with the support to form the oxygenates detected on the fresh catalysts.

3.4.2. *Effect of CO*

A reduced sample of $\text{Rh}(0.6)/\text{La}_2\text{O}_3$ was exposed to a flowing reacting mixture (9% CO, 27% H_2O , 64% Ar) at 673 K during 3 h. Then, the H_2O flow was shut off and only CO and Ar were fed for 24 h. When the water flow was restored after feeding only 9% CO in Ar for 24 hours, a decrease of 90% in the activity was observed. After this experiment, the used solid was characterized using Laser Raman Spectroscopy and intense graphitic carbon bands at 1590 and 1340 cm^{-1} were observed. Feeding only

CO/Ar at 673 K the Boudouard reaction was favored. This reaction involves the disproportionation of carbon monoxide into carbon dioxide and carbon. Since this is an exothermic reaction, it is favored at lower temperatures in the absence of steam.

3.4.3. Effect of an inert and O₂

If formate type species and/or carbonates formed during reaction block the active sites and progressively deactivate the catalyst, its elimination should significantly restore the catalytic activity. To verify this, the reduced catalyst was exposed to the reacting mixture (9% CO, 27% H₂O, 64% Ar (H₂O/CO=3:1)) at 673 K during 20 h. Afterwards, air was fed for a period of 60 min at the same temperature. Then, the catalyst was reduced and the reacting mixture was fed again to observe the effect of the oxygen treatment upon the reaction rate.

In the first part of Figure 7, it is clearly seen that when the reactant stream is restored after flowing Ar for 24 h at 673 K, the catalytic activity remains unchanged. This behavior indicates that the deactivating compounds formed during reaction are not removed by the inert gas (*vide infra*).

The last part of Figure 7 shows that after flowing air at 673 K and subsequent reduction, the catalyst activity was recovered reaching 92% of the initial rate. After that, the Rh(0.6)/La₂O₃ solid deactivated progressively on stream following a similar trend to that observed in the first 3 h on stream

A similar experiment was carried out using the DRIFTS technique. This DRIFTS experiment was designed to investigate the fate of the oxygenates after treating the used catalyst with either He or diluted O₂. The two lowest IR spectra (Fig. 8) show that flowing He at 673 K does not affect the 2500/2870 cm⁻¹ bands. However, these bands disappear after a 10 min exposure to diluted O₂.

Combining the results shown in Figures 7 and 8, it is concluded that the oxygen treatment eliminates the formate and/or carbonate species that would be blocking the active sites and which would be responsible for the progressive deactivation of the Rh(0.6)/La₂O₃ catalyst.

3.5. Effect of the support upon the stability of Rh formulations

Rh supported on $\text{La}_2\text{O}_3\cdot\text{SiO}_2$ is very stable while Rh on La_2O_3 continuously deactivates during 50 h on stream. The main difference the IR spectra show is the absence of oxygenates in the former while they are clearly seen on the latter.

The results reported here show that on Rh/ La_2O_3 :

- i) Adsorbed CO reacts with surface hydroxyls to produce adsorbed formates and oxycarbonates.
- ii) These oxygenates are stable and cannot be desorbed by flowing an inert gas at the reaction temperature of 673 K.
- iii) The 2870 and 2500 cm^{-1} bands disappear upon flowing 5% O_2/He at 673 K and the WGS activity is recovered.
- iv) The steam treatment also eliminates the oxygenates and increases the catalytic activity

(Fig. 4).

These results are now analyzed in terms of the current literature. Shido and Iwasawa [20] concluded that the formate decomposition is the rate determining step on Rh/ CeO_2 . Jacobs et al. [22] arrived at the same conclusion on Pt/ CeO_2 catalysts. Vignatti et al. [27] studied the WGS reaction over Pt/Ce-Zr with varying Ce-Zr compositions. They reported that the catalytic activity decreased with increasing stability of the formate intermediate. They showed that the CH formate vibration increased from 2841 to 2868 cm^{-1} as the ZrO_2 loading varied between 0 and 100%. After purging with Ar at 523 K, they observed that the formate band disappeared in the most active catalysts while it stayed unmodified on the less active ones.

Tabakova et al. [28] also observed that the formation and evolution of the bands typical of formate species at increasing temperature (>573 K) under WGS reaction conditions over nanosized IB group/Ceria catalysts confirm their role as intermediates. These authors concluded that the correlation between the stability of formates and the WGS reaction activity suggests that the decomposition of formates is the rate-limiting step.

Liu et.al [12] reported that the deactivation of the Pt/CeO₂ WGS catalyst (523-623 K) is due to the formation of carbonates on the catalyst surface. In this case, the carbonates cover the CeO₂ surface, block the Pt metal surface, and exert effects on the Pt metal electronic properties.

Masuda [25] studied the stability of La formate in flowing N₂ at increasing temperatures up to 1100 K and found that the CH stretching signal was no longer detectable at 873 K. The sequence of decomposition products are monoxyformate and then oxycarbonates that decompose to La₂O₃ + CO₂ between 873 K and 1043 K. Another piece of information consistent with the increase of catalytic activity after water pretreatment (Fig. 1) is the increased lability of formates in humid environment [21]. This overall picture is also consistent with the fact that both formates and carbonates are present on Rh(0.6)/La₂O₃ while they are absent in the very stable more acidic Rh(0.6)/La₂O₃.SiO₂ (La₂Si₂O₇.SiO₂) formulation.

In view of the results of other authors [12,25-27] and those reported here, the deactivation of Rh/La₂O₃ could be caused by the high stability of the oxygenates being strongly retained on the active sites. Only those treatments with diluted O₂ or steam are effective to either burn or decompose them, thus restoring the catalytic activity.

4. Conclusions

The “operando” DRIFTS experiments show that under WGS reaction conditions at 673 K, the detectable surface species are completely different on Rh(0.6)/La₂O₃ and Rh(0.6)/La₂O₃(27).SiO₂. On the former, strong and stable signals of oxycarbonates are observed while they are absent in the latter. This is also confirmed by XRD that additionally shows that the La₂O₃.SiO₂ support is made up of La₂Si₂O₇ and SiO₂ with no free La₂O₃. A significant difference from the catalytic standpoint is the presence of oxygenate bands that increase with both reaction temperature and time-on-stream over Rh(0.6)/La₂O₃. Either formates, carbonates or both slowly cover the active sites and therefore progressively deactivate the Rh(0.6)/La₂O₃ formulation.

The different stability of Rh/La₂O₃ and Rh/La₂Si₂O₇.SiO₂ is due to the different basicity of the supports. When the support is too basic, as La₂O₃ is, the stability of the formates and carbonates significantly increases. This process leads to a slow but steady deactivation of this solid and the activity is recovered when both the formates and the newly formed carbonates are either decomposed by the steam treatment at 673 K or eliminated by flowing 5% O₂/He at the same temperature.

5. Acknowledgments

The authors acknowledge the financial support received from UNL, CONICET, ANPCyT and the “Fonds National de la Recherche Scientifique (FNRS)” of Belgium. They also wish to thank the SECyT (Argentina)—FNRS (Belgium) program that allowed us to develop this collaborative effort. Thanks are also given to the Japan International Cooperation Agency (JICA) for the donation of the XRD equipment; to ANPCyT for the purchase of the Raman instrument (PME 87-PAE 36985) and to Elsa Grimaldi for the English language editing.

6. References

- [1] P. Liu, J.A. Rodriguez, Y. Takahashi, K. Nakamura, *J. Catal.* 262 (2009) 294–303.
- [2] Y. Li, Q. Fu, M. Flytzani – Stephanopoulos, *Appl. Catal. B: Environ.* 27 (2000) 179–191.
- [3] A.F. Ghenciu, *Curr. Opin. Solid State Mater. Sci.* 6 (2002) 389-399.
- [4] H. Li, A. Goldbach, W.Z. Li, H.Y. Xu, *J. Membr. Sci.* 299 (2007) 130.
- [5] C. Ratnasamy, J.P. Wagner, *Catal. Rev.* 51 (2009) 325–440.
- [6] J.A. Francesconi, M.C. Mussati, P. Aguirre, *J. Power Sources* 173 (2007) 467–477.
- [7] J.F. Múnera, S. Irusta, L.M. Cornaglia, E.A. Lombardo, D. Vargas Cesar, M. Schmal, *J. Catal.* 245 (2006) 25-34.
- [8] C.A. Cornaglia, J.F. Múnera, E.A. Lombardo, *Ind. Eng. Chem. Res.* 50 (2011) 4381–4389.
- [9] X. Wang, R.J. Gorte, J.P. Wagner, *J. Catal.* 212 (2002) 225-230.

- [10] A. Goguet, R. Burch, Y. Chen, C. Hardacre, P. Hu, R.W. Joyner, F.C. Meunier, B.S. Mun, D. Thompsett, D. Tibiletti, *J. Phys. Chem. C* 111 (2007) 16927-16933.
- [11] A. Goguet, F. Meunier, J.P. Breen, R. Burch, M.I. Petch, A. Faur Ghenciu, *J. Catal.* 226 (2004) 382-392.
- [12] X. Liu, W. Reuttinger, X. Xu, R. Farrauto, *Appl. Catal. B* 56 (2005) 69-75.
- [13] S. Hilaire, X. Wang, T. Luo, R. T. Gorte, J.P. Wagner, *Appl. Catal. A: Gen.* 215 (2001) 271-278.
- [14] D. Martin, D. Duprez, *Appl. Catal. A: General* 131 (1995) 297-307.
- [15] S. Irusta, J. Múnera, C. Carrara, E.A. Lombardo, L.M. Cornaglia, *Appl. Catal. A* 287 (2005) 147-158.
- [16] H. Vidal, S. Bernal, R. Baker, G.A. Cifredo, D. Finol, J.M. Rodríguez-Izquierdo, *Appl. Catal. A* 208 (2001) 111-123.
- [17] P. Panagiotopoulou, D.I.Kondarides, *Catal. Today* 112 (2006) 49-52.
- [18] H. Vidal, S. Bernal, R. Baker, D. Finol, J.A. Perez Omil, J.M. Pintado, J.M. Rodríguez-Izquierdo, *J. Catal.* 183 (1999) 53-62.
- [19] G. Blanco, M.A. Calvino, M.A. Cauqui, G.A. Cifredo, J.A. Pérez, *J. Alloys Compd.* 207 (1994) 201-205.
- [20] M. Mihaylov, E. Ivanova, Y. Hao, K. Havjiivanov, H. Knozinger, B.C. Gates, *J. Phys. Chem, C* 112 (2008) 18973-18983.
- [21] T. Shido, Y. Iwasawa, *J. Catal.* 141 (1993) 71-81.
- [22] G. Jacobs, U.M. Graham, E. Chenu, P.M. Patterson, A. Dozier, B.H. Davis, *J. Catal.* 229 (2005) 499-512.
- [23] E. Chenu, G. Jacobs, A.C. Crawford, R.A. Keogh, P.M. Patterson, D.E. Sparks, B.H. Davis, *Appl. Catal. B: Environ.* 59 (2005) 45-56.
- [24] S. Lacombe, C. Geantet, C. Mirodatos, *J. Catal.* 151 (1994) 439.
- [25] Y. Masuda, *Thermochím. Acta* 67 (1983) 271-285.

- [26] A.N. Shirsat, M. Ali, K.N. Kaimal, S.R. Bharadwaj, D. Das, *Thermochím. Acta* 399 (2003) 167-170.
- [27] C.I. Vignatti, M.S. Avila, C.R. Apesteguía, T.F. Garetto, *Catal. Today* 171 (2011) 297-303.
- [28] T. Tabakova, F. Boccuzzi, M. Manzoli, J.W. Sobczak, V. Idakiev, D. Andreeva, *Appl. Catal. A: Gen.* 298 (2006) 127-143.

Accepted Manuscript

Figure captions

Figure 1. (a): DRIFT spectra obtained during WGS reaction with 1.1% H₂O + 1.1% CO + 98.8% He on Rh(0.6)/La₂O₃(27).SiO₂ at different temperatures and 1 atm, referenced to the spectrum of the reduced catalyst prior to reactant admission. **(b):** Recorded mass spectrometer signals.

Figure 2. Time evolution of DRIFT spectra obtained during the WGS reaction with 1.1% H₂O, 1.1% CO, 98.8% He on Rh(0.6)/La₂O₃ at 673 K and 1 atm, referenced to the spectrum of the reduced catalyst prior to gas admission.

Figure 3. (a): DRIFT spectra recorded during WGS reaction with 1.1% H₂O, 1.1% CO, 98.8% He (H₂O/CO=1:1) on Rh(0.6)/La₂O₃ at different temperatures (323-673K) and atmospheric pressure, referenced to spectrum of the reduced catalyst prior to gas admission. **(b):** Mass spectrometer signals recorded during the WGSR.

Figure 4. Steam treatment enhances the Rh(0.6)/La₂O₃ activity. (a): Reaction at 673 K, 9% CO, 27% H₂O, 64% Ar, W/F=2.65x10⁻⁷ g h ml⁻¹.

Figure 5. IR spectra of Rh(0.6)/La₂O₃ catalyst: (a) fresh catalyst. (b) after WGS reaction during 24 h at 673 K. (c) after WGS reaction for 1h followed to a exposure of 27 % H₂O/Ar during 24 h.

Figure 6. Rh(0.6)/La₂O₃. The water treatment (1.1 % H₂O in He) diminish the oxygenates bands and WGSR increases them at 673 K. WGS feed composition: 1.1% H₂O, 1.1% CO, 98.8% He.

Figure 7. Effect of Ar and air + H₂ treatment over the Rh(0.6)/La₂O₃ catalyst activity. Reaction at 673K, feed 9% CO, 27% H₂O, 64% Ar.

Figure 8. DRIFTS results after treatment with oxygen at 673 K, O₂(5%)/He. WGS feed composition: 1.1% H₂O, 1.1% CO, 98.8% He. Spectra referenced to the spectrum of the reduced catalyst prior to gas admission.

Table 1. Stability test of Rh(0.6)/La₂O₃ at 673 K, H₂O:CO=3:1, 1 atm, W/F= 2.65.10⁻⁷ g h ml⁻¹ *

time [h]	1	10	20	30	40	50
r _{CO} x10 ⁴ [mol g ⁻¹ s ⁻¹]	2.65	1.90	1.75	1.50	1.35	1.3

*For the Rh(0.6)/La₂O₃(27).SiO₂ catalyst, r_{CO} x10⁴ = 1.65 mol g⁻¹ s⁻¹ (constant for at least 50 h).

Accepted Manuscript

Table 2. WGS turnover frequencies of supported noble metal catalysts

	Rh dispersion (%) ⁽¹⁾	Initial rate at 400°C (x10 ⁴ mol g ⁻¹ s ⁻¹)	TOF at 400°C (s ⁻¹)	Ref
Rh(0.6)/La ₂ O ₃	14	2.65	53.1	This work
Rh(0.6)/La ₂ O ₃ .SiO ₂	79	1.65	6.0	This work
Pt(0.5)/SiO ₂			0.1	[17] ⁽²⁾
Pt(0.5)/MgO			0.4	[17] ⁽²⁾
Pd(0.5)/CeO ₂			1.0	[17] ⁽²⁾
Pd(0.5)/Al ₂ O ₃			0.2	[17] ⁽²⁾

⁽¹⁾ Calculated from H₂ chemisorption

⁽²⁾ Calculated using a feed stream of 3% CO and 10% H₂O (balance He)

Table 3. Phases observed in both catalysts, fresh and used, through XRD and LRS.

Solids	Reflections (2 θ) ^(*)	Raman 200-1600 cm ⁻¹ region
Rh(0.6)/La₂O₃ fresh		
La(OH) ₃ (main)	15.7, 27.4, 28.0, 39.6, 48.7	274, 339, 447, 597
Ia-La ₂ O ₂ CO ₃ (trace)	13.1, 22.8, 29.5, 30.8, 31.3	294, 315, 340, 356, 387, 437(sh), 450, 1057, 1089
II-La ₂ O ₂ CO ₃ (trace)	22.2, 25.8, 30.4, 42.5, 44.4, 47.5	358, 384, 747, 1086
Rh(0.6)/La₂O₃ used^(a)		
II-La ₂ O ₂ CO ₃	22.2, 25.2, 25.8, 27.6, 30.4, 42.5, 44.4, 47.5, 50.3, 54.8, 56.9	358, 384, 747, 1086
graphite	undetected	1340, 1590 (only in used, weak)
Rh(0.6)/La₂O₃(27).SiO₂ fresh and used^(a)		
La ₂ Si ₂ O ₇	28, 45 (broad peaks)	No signals
graphite	undetected	1340, 1590 (only in used, weak)

^(*)Most intense reflections.

^(a)After WGS, feeding 9% CO, 27% H₂O, 64% Ar at 673K for 24 h.

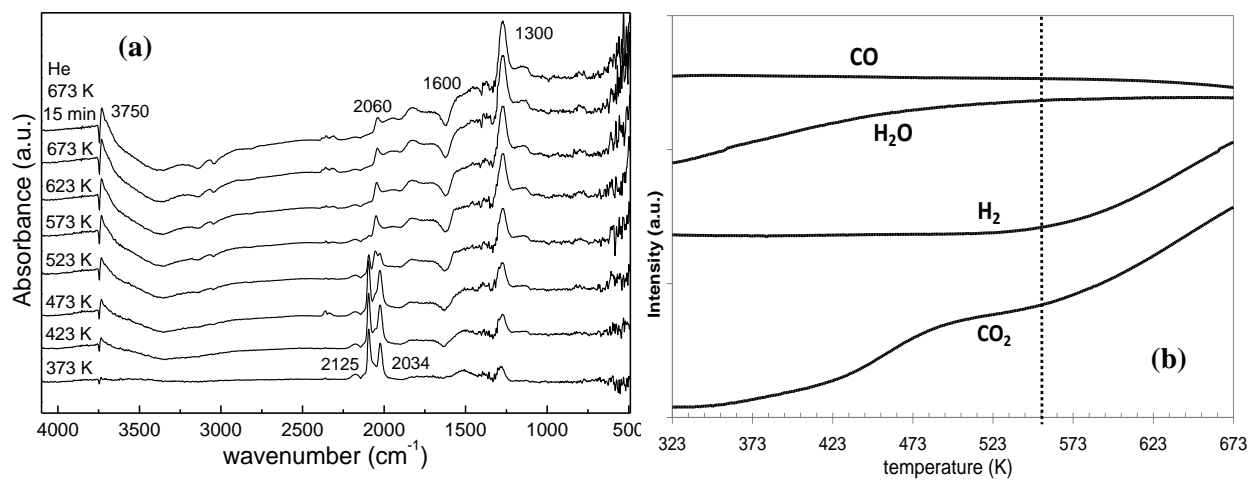
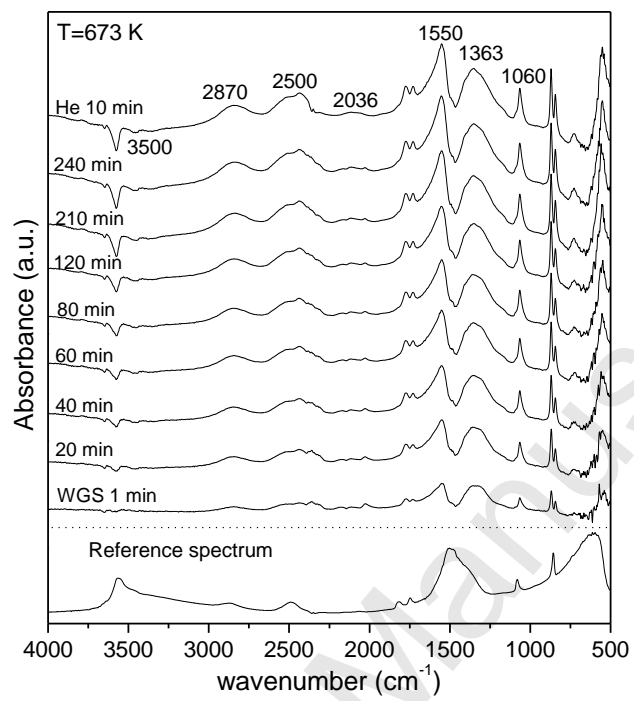


Figure 1

**Figure 2**

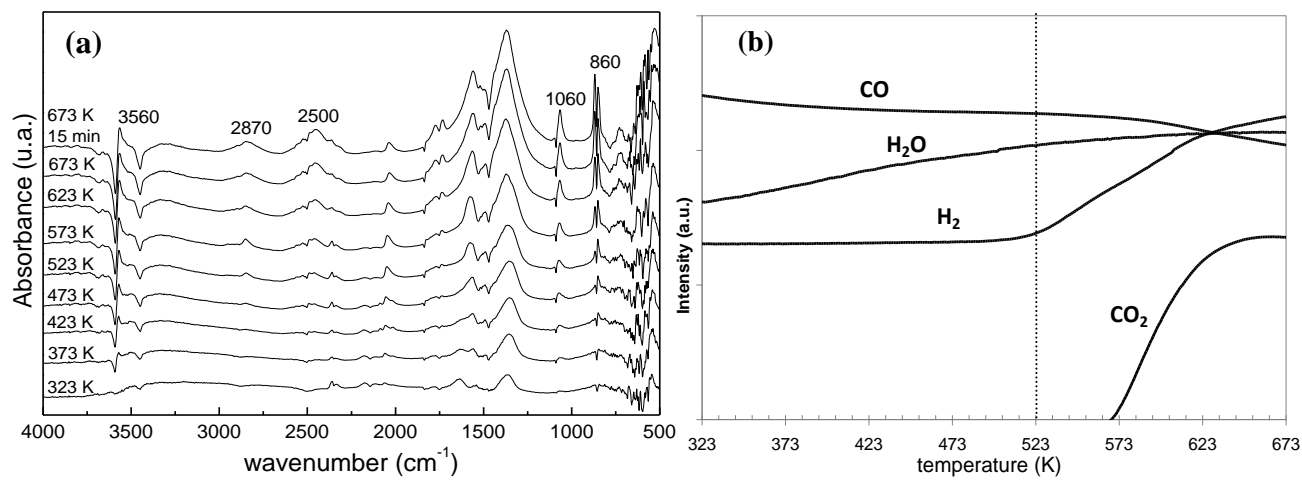
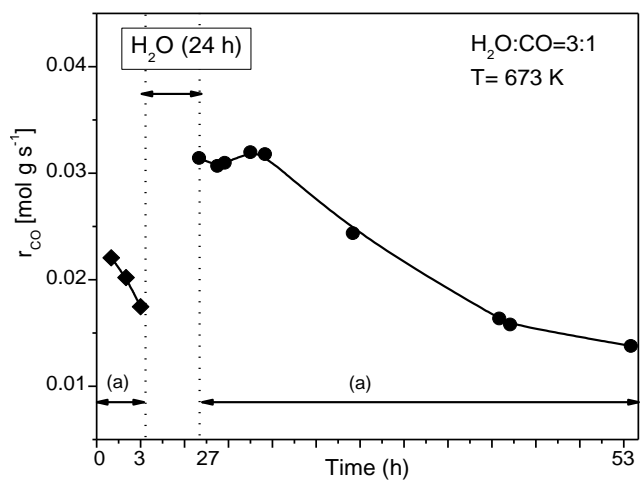


Figure 3

**Figure 4**

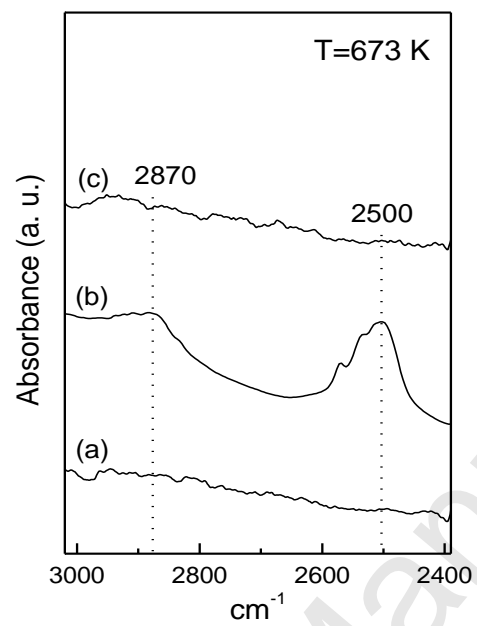
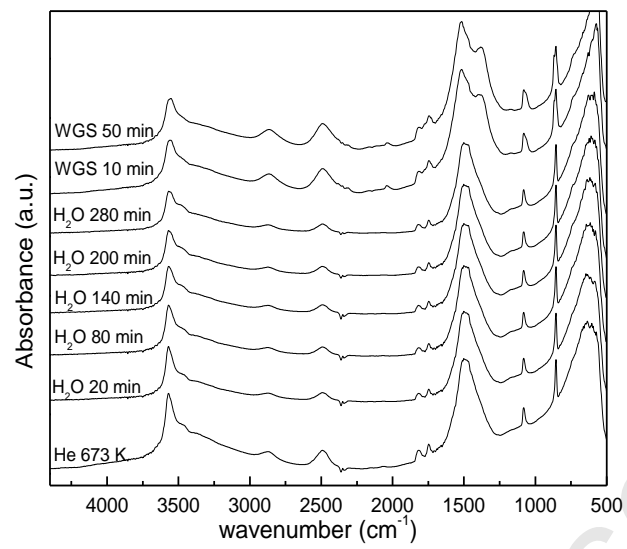


Figure 5

**Figure 6**

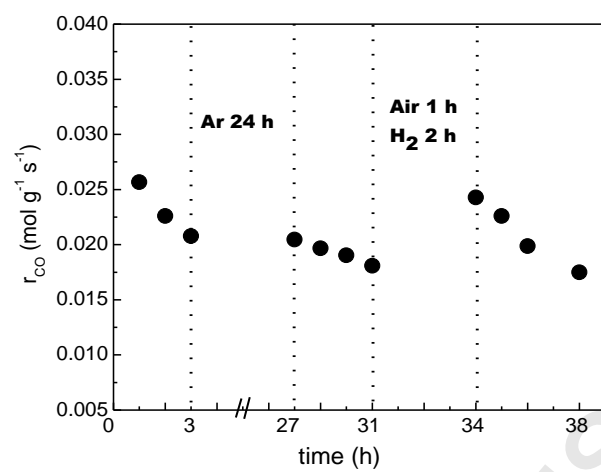


Figure 7

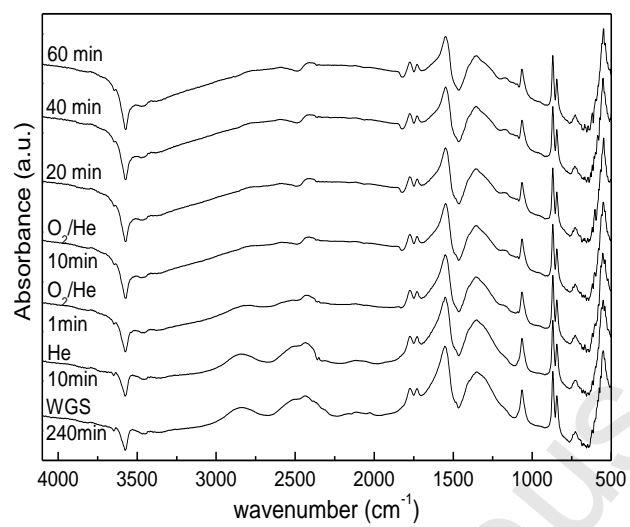


Figure 8